Mon. Not. R. Astron. Soc. 425, 757-762 (2012)



The exoplanet eccentricity distribution from Kepler planet candidates

Stephen R. Kane,* David R. Ciardi, Dawn M. Gelino and Kaspar von Braun

NASA Exoplanet Science Institute, Caltech, MS 100-22, 770 South Wilson Avenue, Pasadena, CA 91125, USA

Accepted 2012 June 28. Received 2012 June 28; in original form 2012 May 29

ABSTRACT

The eccentricity distribution of exoplanets is known from radial velocity surveys to be divergent from circular orbits beyond 0.1 au. This is particularly the case for large planets where the radial velocity technique is most sensitive. The eccentricity of planetary orbits can have a large effect on the transit probability and subsequently the planet yield of transit surveys. The *Kepler* mission is the first transit survey that probes deep enough into period space to allow this effect to be seen via the variation in transit durations. We use the *Kepler* planet candidates to show that the eccentricity distribution is consistent with that found from radial velocity surveys to a high degree of confidence. We further show that the mean eccentricity of the *Kepler* candidates decreases with decreasing planet size indicating that smaller planets are preferentially found in low-eccentricity orbits.

Key words: techniques: photometric – techniques: radial velocities – planetary systems.

1 INTRODUCTION

Planets discovered using the radial velocity (RV) method have dominated the total exoplanet count until recently, when the transit method has made increasing contributions. The long time baseline of RV surveys has allowed the detection of more diverse orbital geometries than achievable by ground-based transit surveys. The Kepler mission, however, with its multi-year baseline, can begin to probe into parameter space previously reserved for RV studies. At longer periods, orbits tend to diverge significantly from the circular case beyond a semi-major axis of ~ 0.1 au (Butler et al. 2006), although there may be small observational biases that skew this distribution (Shen & Turner 2008). This insight has led to numerous attempts to account for eccentricity in the context of planet formation and orbital stability (Ford & Rasio 2008; Jurić & Tremaine 2008; Matsumura, Takeda & Rasio 2008; Malmberg & Davies 2009; Wang & Ford 2011) and the influence of tidal circularization (Pont et al. 2011).

It has been shown how eccentricity distribution effects transit probabilities (Kane & von Braun 2008, 2009) and projected yields of transit surveys (Barnes 2007; Burke 2008). This influence is minor for the ground-based surveys since they are primarily sensitive to giant planets in short-period orbits. However, the *Kepler* mission is expected to be impacted by this distribution since it probes out to much longer periods with a much reduced disadvantage of a window function that affects observations from the ground (von Braun, Kane & Ciardi 2009). A comparison of the *Kepler* results in the context of eccentricity and transit durations with the RV

distribution has been suggested by Ford, Quinn & Veras (2008) and Zakamska, Pan & Ford (2011) and carried out by Moorhead et al. (2011), but initial planet candidate releases by the Kepler project do not provide enough period sensitivity (Borucki et al. 2011a,b). The most recent release of *Kepler* planet candidates by Batalha et al. (2012) increases the total number of candidates to more than 2300 and the time baseline probed to beyond 560 d. This has several implications for studies of eccentricity distributions. The Kepler mission is sensitive to planets significantly smaller than those accessible by current RV experiments and thus allows a more indepth study of the dependence of eccentricity on the planet mass/size and multiplicity. If the eccentricity distributions of Kepler and RV planets were found to be substantially different, then this would reveal a selection effect in the way Kepler candidates are selected which is biased against eccentric orbits. A direct comparison of the two distributions, provided they are consistent for the planet mass/size region where their sensitivities overlap, will allow a more exhaustive investigation of orbital eccentricity to be undertaken.

Here we present a study of the eccentricity distribution of planets discovered with the RV method and the complete list of *Kepler* planet candidates. We calculate expected transit durations for circular orbits and compare them with either calculated or measured eccentric transit durations (Section 2). Our results show that the measured transit durations from RV data (Section 3) and the *Kepler* candidates (Section 4) are consistent with having the same distribution. We estimate the impact parameter distribution for the *Kepler* candidates and show that their mean eccentricity decreases with decreasing planet size (Section 5), which supports the hypothesis that smaller planets tend to be found in multiple systems in near-circular orbits. We discuss additional astrophysical aspects in Section 6 and conclude in Section 7.

^{*}E-mail: skane@ipac.caltech.edu

2 ECCENTRICITY AND TRANSIT DURATION

A concise description of exoplanetary transit modelling and associated parameters is presented elsewhere (Mandel & Agol 2002; Seager & Mallén-Ornelas 2003). Here we concentrate on the relevant details to our analysis: transit duration and eccentricity. The transit duration for a circular orbit is given by

$$t_{\rm circ} = \frac{P}{\pi} \arcsin\left(\frac{\sqrt{(R_{\star} + R_{\rm p})^2 - a^2 \cos^2 i}}{a}\right),\tag{1}$$

where P is the orbital period, a is the semi-major axis, i is the orbital inclination, and R_{\star} and $R_{\rm p}$ are the stellar and planetary radii, respectively. The impact parameter of a transit is given by

$$b \equiv \frac{a}{R} \cos i \tag{2}$$

and is defined as the projected separation of the planet and star centres at the point of mid-transit.

For an eccentric orbit, the star-planet separation r is time dependent and is given by

$$r = \frac{a(1 - e^2)}{1 + e\cos f},\tag{3}$$

where e is the orbital eccentricity and f is the true anomaly. Replacing a with r at the time of inferior conjunction in equations (1) and (2) provides generalized expressions for transit duration and impact parameter for non-circular orbits. Burke (2008) converts these expressions into the scaling factor

$$\frac{t_{\rm ecc}}{t_{\rm circ}} = \frac{\sqrt{1 - e^2}}{1 + e\cos(\omega - 90^\circ)},\tag{4}$$

where ω is the periastron argument of the orbit.

3 RADIAL VELOCITY ECCENTRICITY DISTRIBUTION

We first investigate the eccentricity distribution of the planets discovered with the RV technique and the subsequent impact on the predicted transit duration. The Exoplanet Data Explorer (EDE)¹ stores information only for those planets that have complete orbital solutions and thus are well suited to this study (Wright et al. 2011). The EDE data are current as of 2012 February 24 and include 204 planets after the following criteria are applied: $\log g > 3.5$ to exclude giant stars and a < 1.5 au to produce a sample that covers the same region in parameter space as the *Kepler* candidates.

To calculate the transit duration, one needs an estimate of the planetary radius. For planets that are not known to transit, we approximate the planetary radius using the simple model described by Kane & Gelino (2012). This model adopts a radius of 1 Jupiter radius for masses $\geq 0.3 M_{\rm Jupiter}$ and utilizes a power-law fit to the masses and radii of the known transiting planets for masses $< 0.3 M_{\rm Jupiter}$. In order to estimate the radius of the host star, we use the following relation related to the surface gravity:

$$\log g = \log \left(\frac{M_{\star}}{\mathrm{M}_{\odot}} \right) - 2 \log \left(\frac{R_{\star}}{\mathrm{R}_{\odot}} \right) + \log g_{\odot}, \tag{5}$$

where $\log g_{\odot} = 4.4374$ (Smalley 2005). Using the equations of Section 2 and the measured orbital parameters, we calculate the transit duration for both the circular and eccentric cases. We then

take the absolute value of the difference between the two durations as a diagnostic for the eccentricity distribution.

The top-left panel of Fig. 1 shows the eccentricity distribution of the RV planets taken from EDE as a function of a. The distribution begins to diverge from mostly circular orbits beyond 0.04 au, and by 0.1 au it has an eccentricity range of 0.0–0.5. This distribution is widely attributed to tidal damping of the orbits after the disc has dissipated. According to Goldreich & Soter (1966), the time-scale for orbital circularization is $\propto a^{6.5} M_{\star}^{-1.5}$, where M_{\star} is the stellar mass. Note that the two planets inside of 0.04 au with e > 0.1 are GJ 436b and GJ 581e, both of which have M dwarf host stars.

The other three panels in Fig. 1 show the calculated duration difference by Δt as a function of a. Δt is the absolute value of the difference between the calculated transit duration for a circular orbit and the calculated transit duration based upon the measured orbital parameters (i.e. $\Delta t = |t_{\rm circ} - t_{\rm ecc}|$), which is indicative of the divergence from the assumption of only circular orbits. The top-right panel assumes edge-on orbits ($i = 90^\circ; b = 0$) for both the circular and eccentric cases. We show the effect of increasing the impact parameter of the transits for b = 0.5 and b = 0.8. The mean of Δt is not significantly changed except for relatively high values of b. We evaluate the significance of this distribution in the following section.

It should be noted that, in order for a transit to take place, i can at most deviate only slightly from 90° . The consequent small angle approximation means that the uniform distribution of i values maps to a uniform distribution of b values, making all values of b equally likely to occur.

4 ANALYSIS OF KEPLER TRANSIT DURATIONS

The release of more than 2300 Kepler candidates is described in detail by Batalha et al. (2012). The appendix table that contains the characteristics of the Kepler candidates was extracted from the NASA Exoplanet Archive.² We perform a similar calculation for Δt as described in the previous section. However, this time we calculate the difference between $t_{\rm circ}$ and the duration measurement provided by the candidates table, t_{kepler} . We do not use the provided b values since they are based on a circular orbit assumption from the measured transit duration and the stellar radii. We thus make no assumption on the value of b. We require $R_{\star} > 0.7 \,\mathrm{R}_{\odot}$ to remove candidates for which the uncertainty in the stellar radius determination contributes significantly to the uncertainty in the transit duration. We also include only those candidates for which $R_p > 8 R_{\oplus}$ to limit the sample to giant planets, similar to the RV sample. We show Δt versus a for the 176 resulting candidates in the left-hand panel of Fig. 2.

To compare this distribution to its equivalents in Section 3 we perform a null hypothesis Kolmogorov–Smirnov (KS) test to assess the statistical significance of their similarities. We binned the data by Δt into 40 equal bins of 0.5 to collapse the data into one-dimensional samples. The right-hand panel of Fig. 2 shows the normalized cumulative histograms for each of the four distributions: the three KS tests compare the *Kepler* candidates to the RV planets with assumed b = 0.0 (Test 1), b = 0.5 (Test 2) and b = 0.8 (Test 3). Test 1 produces a KS statistic of D = 0.05 that indicates a 100 per cent probability that these data are consistent with being drawn from the same distribution (the null hypothesis). Test 2 produces a similar

¹ http://exoplanets.org/

² http://exoplanetarchive.ipac.caltech.edu/

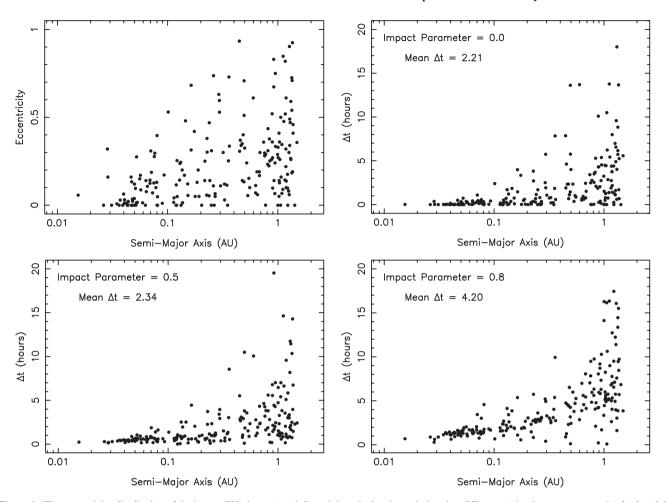


Figure 1. The eccentricity distribution of the known RV planets (top-left) and the calculated transit duration difference (circular versus eccentric) for b = 0.0 (top-right), 0.5 (bottom-left) and 0.8 (bottom-right). See Section 3 for details.

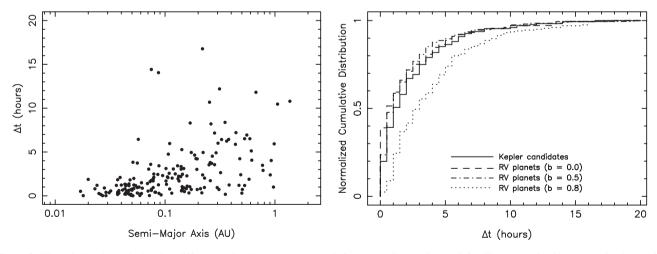


Figure 2. The calculated transit duration difference (circular versus measured) for the *Kepler* candidates (left). The cumulative histograms for the *Kepler* candidates and the three RV planets shown in Fig. 1 show a close match between the distributions, quantified by the KS test described in Section 4.

result of D = 0.075, also a probability of 100 per cent. Test 3 results in D = 0.2 which is equivalent to a probability of 36 per cent. This result can readily be seen in the right-hand panel of Fig. 2 where the b = 0.0 and b = 0.5 cases are almost indistinguishable from the *Kepler* candidates, but the b = 0.8 case is clearly discrepant. As mentioned in Section 3, the small range of values for i for transits

results in a uniform distribution of impact parameters with a mean of b=0.5. The statistical congruence in the KS test implies that the *Kepler* mission is indeed recovering the eccentricity distribution of the RV planets.

A criticism that may be levelled at this methodology is that the outcome of the statistical test depends upon the manner in which the

Table 1. Minimum eccentricities for selected candidates.

KOI	Period (d)	t _{kepler} (h)	Δ <i>t</i> (h)	$e_{ m min}$
44.01	66.47	19.74	12.2	0.74
211.01	372.11	4.81	10.5	0.82
625.01	38.14	4.24	10.7	0.85
682.01	562.14	9.49	10.8	0.64
1230.01	165.72	27.26	11.8	0.34
1894.01	5.29	8.80	14.4	0.75
2133.01	6.25	11.26	14.1	0.67
2481.01	33.85	14.95	16.8	0.64

data are binned. To determine the robustness of our results, we used both half and double the number of bins to change the resolution of the sampling. For half the number of bins, we obtain D=0.1 (100 per cent), D=0.1 (100 per cent) and D=0.2 (77 per cent) for Tests 1, 2 and 3, respectively, as described above. If we then double the number of bins, the results are D=0.05 (100 per cent), D=0.0375 (100 per cent) and D=0.1625 (22 per cent) for Tests 1, 2 and 3, respectively. Clearly the results for Tests 1 and 2 are consistent with previous results and the results for Test 3 retain their discrepancies though with a variety of values. As described earlier, Test 3 (b=0.8) is the least relevant of the results since the mean impact parameter is b=0.5.

Finally, we investigate a sample of the outliers with particularly large deviations from the circular model ($\Delta t > 10$ h). These candidates are shown in Table 1. Since the *Kepler* data frequently do not contain any secondary eclipse, e and ω are unknown. We calculate the transit duration $t_{\rm ecc}$ as a function of e and ω via equation (4). We then produce a grid of $|t_{\rm circ} - t_{\rm kepler}|/|t_{\rm circ} - t_{\rm ecc}|$ for all values of e and ω . Locations where the grid values are approximately equal to 1 are possible solutions for which the measured transit duration in the *Kepler* candidate catalogue is consistent with certain values of e and ω .

An example of this is shown in Fig. 3 where we present results of the above calculations as an intensity map for KOI 1230.01.

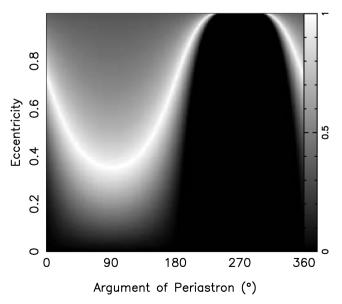


Figure 3. An intensity map for KOI 1230.01 that shows the result of dividing Δt using t_{kepler} by Δt using t_{ecc} . Thus, a value of 1 (peak intensity) corresponds to the best solution (Section 4).

In order to be compatible with the *Kepler* measured duration, the eccentricity of the planet must be at least 0.34. This process is repeated for each of the candidates in Table 1 in which we report the minimum required eccentricity e_{\min} for each candidate. It is worth noting, however, that these minimum eccentricities are not singular values but rather distributions, as can be seen by the grey scale in Fig. 3. The uncertainties depend highly upon the various random errors in the measured values of the *Kepler* candidates catalogue, including *i*. For example, the stellar radius of KOI 2481.01 would need to be \sim 45 per cent of the catalogue value in order for it to be in a circular orbit and the duration discrepancy to be reduced to zero.

Further of interest in Table 1 are the relatively short-period planets KOI 1894.01 and KOI 2133.01. One normally expects a transit duration of several hours for period such as these. However, the values of $t_{\rm kepler}$ and Δt shown in this table imply a $t_{\rm circ}$ larger than 20 h! This does not appear to make sense until one considers the stellar radius. Note from equation (1) that, for an edge-on orbit and small $R_{\rm p}$, the transit duration scales linearly with the size of the star. For these two candidates, the stellar radii are 8.6 and $9.3\,{\rm R}_{\odot}$, respectively, thus resulting in a large Δt and a significant eccentricity required to be consistent with observations. Note, however, that we have assumed b=0. As one increases the impact parameter, the predicted transit duration will decrease and thus become closer to its measured value. Results for individual cases extracted from the global distribution, such as those in Table 1, must therefore be treated with caution.

5 PLANET SIZE CORRELATION

We mentioned in Section 4 that the analysis of the *Kepler* objects included only candidates for which $R_{\rm p}>8\,{\rm R}_{\oplus}$. Here we perform a separate study by repeating the calculations of Δt for the *Kepler* candidates for a range of planetary radii. We allow the candidate sample to include all radii larger than $1\,{\rm R}_{\oplus}$ to $8\,{\rm R}_{\oplus}$ and calculate the mean of the Δt distribution in each case. We show our results in Fig. 4.

An interpretation of this figure is that the eccentricity distribution of exoplanets remains relatively flat until we probe below planets the size of Neptune. At that point the eccentricity distribution of the orbits becomes rapidly and significantly more circular. This is not unexpected since we understand from the Solar system that the inefficiency of tidal dissipation (the quality factor *Q*) is much larger

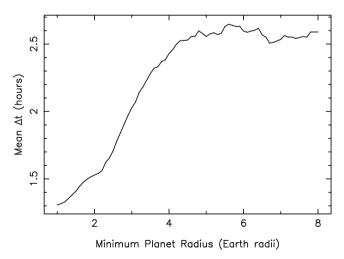


Figure 4. The mean Δt for the *Kepler* candidates as a function of the minimum planetary radius included in the sample (Section 5).

for high-mass than for low-mass planets (Goldreich & Soter 1966), resulting in shorter tidal circularization time-scales for smaller planets. One aspect of the *Kepler* candidate sample that may influence this result is that they are dominated by planets at smaller semimajor axes since these have much larger transit probabilities. As indicated by Lissauer et al. (2011b, 2012), multi-planet systems comprise a large proportion of the total *Kepler* candidate sample and these systems in particular are less prone to be false positives. The findings that planet occurrence increases with decreasing planet mass (see for example Howard et al. 2010) then suggests that smaller planets find stable architectures in systems with circular orbits and without large planets in eccentric orbits. This lends credence to two scenarios: (1) core accretion forming terrestrial planets in circular orbits, and (2) disc instability and capture scenario explaining the existence of giant planets in eccentric orbits.

A potential alternative explanation for the dependence of Δt upon $R_{\rm planet}$ is a correlation between planetary radii and semi-major axes in the *Kepler* sample due to completeness. Smaller planets in closer orbits would be more likely to have had their orbits circularized leading to their domination of the sample. We do not, however, see such an effect but instead find no correlation between planet size and period in the *Kepler* catalogue for the selected range of orbital periods. Thus, we conclude that this effect is not the cause of the observed radius/eccentricity correlation.

6 DISCUSSION

There are various sources of potential systematic noise inherent in the data used to perform this analysis. For example, we have not taken the stellar limb darkening into account when considering transit durations. However, since we only consider the total transit duration (first contact to last contact), this will be a negligible effect.

For the Kepler candidates, the primary source of uncertainty arises from the stellar parameters that are used to derive many of the planetary candidate parameters. The primary difficulties arise from the stellar radii whose precision is usually worse than ~ 10 per cent, even when spectra are available. Our assumption is that these uncertainties are not significantly biased in one direction of the other and thus only add white noise to the overall statistical properties. One method to test this assumption is to consider multicandidate systems for which a change in the stellar radius will affect all calculated transit durations in a similar way. For example, KOI 157 (Kepler-11) has six detected planet candidates with measured transit durations that are shorter than predicted, and with an estimated host star radius of 1.06 R_{\odot} . Three of those discrepancies are quite small making them almost consistent with a circular orbit, as noted by Lissauer et al. (2011a). Attempting to force circular orbits by reducing the stellar radius slightly makes two of the planets consistent with a circular orbit but leaves the other durations highly discrepant. A more global test of the assumption is the application of a range of uniform scaling factors to the stellar radii to try to produce transit durations consistent with circular orbits for the bulk of the distribution. These corrections did not change the distribution shown in Fig. 2, leading to the conclusion that our calculated Δt values are not affected by systematically incorrect stellar radii.

Considering the uncertainties in the radii of the *Kepler* host stars, our limits on the eccentricities of the specific *Kepler* candidates discussed in Section 4 should be treated in that context. Indeed, this is why we concentrate our comments on the global distribution of all the *Kepler* objects and their parameters, rather than on individual cases. Furthermore, the *Kepler* sample is only complete to ~ 0.5 au with declining completeness beyond this to ~ 1.5 au. Thus, the

number of candidates beyond 0.5 au is smaller but still sufficient for a valid comparison to be made.

One aspect of the *Kepler* candidates that was not taken into account was the multiplicity of the systems. As suggested at the conclusion of the previous section, the multiplicity may indeed play a significant role in stabilizing planets in approximately circular orbits, particularly for those in the low mass/size regime. This is true of the RV planets also, some of which are known to lie in multiple systems of super-Earth mass planets and with relatively circular orbits such as the system orbiting HD 10180 (Lovis et al. 2011).

In Section 1 we mentioned the eccentricity bias found by Shen & Turner (2008) due to low-amplitude signals in RV samples. This is a small but real effect which depends upon the sampling rate and has the consequence of underestimating the number of near-circular orbits. Shen & Turner (2008) develop a figure of merit and find that only $\sim \! 10$ per cent of the planets considered in their sample are affected by this bias. The samples studied here are too small to detect such an effect, but we mention it here as a consideration for future similar work for which the sample sizes and, more particularly, the period range explored have grown substantially.

Finally, a minor impact on the stellar radii that should be noted is the one due to the relation between planet frequency and stellar metallicity. Johnson et al. (2010) explored the mass—metallicity relationship for stars that harbor planets and found a positive correlation of planet frequency with both stellar mass and metallicity, in accordance with the findings of Fischer & Valenti (2005). This positive correlation was also found empirically for M dwarfs by Terrien et al. (2012). For a given stellar mass, a larger metallicity leads to a smaller radius in order to reach hydrostatic equilibrium. The implication for this study is that many of the *Kepler* host stars will have relatively high metallicity leading to an overestimated radius. However, this effect is at the level of a few per cent and not expected to interfere with the results of this study.

7 CONCLUSIONS

By conducting a transit survey that is sensitive to long enough periods, it is expected that one will eventually reproduce the eccentricity distribution found amongst RV planets. This has not been possible until very recently, when the *Kepler* presented a large sample of long-period planets candidates, providing the incentive for this study and a similar one by Plavchan, Bilinski & Currie (2012). For individual planets, the eccentricity may be discerned via asymmetry in the shape of ingress and egress (Kipping 2008). This requires exquisite photometry and is highly sensitive to ω . We have shown here the consistency of the *Kepler* candidates' eccentricity distribution with their RV planets' counterparts. The correlation of eccentricity with planet size is also an expected result based upon the discoveries of small planets in multiple systems and indicates that there is an empirical approach from which to both reverse-engineer formation scenarios and predict future stability patterns.

ACKNOWLEDGMENTS

The authors would like to thank Rory Barnes, Eric Ford, Andrew Howard and Suvrath Mahadevan for several useful discussions. They would also like to thank the anonymous referee, whose comments greatly improved the quality of the paper. This research has made use of the Exoplanet Orbit Database and EDE at exoplanets.org. This research has also made use of the NASA Exoplanet

762 S. R. Kane et al.

Archive, which is operated by the California Institute of Technology, under contract with the National Aeronautics and Space Administration under the Exoplanet Exploration Program.

REFERENCES

Barnes J. W., 2007, PASP, 119, 986

Batalha N. M. et al., 2012, ApJS, preprint (arXiv:1202.5852)

Borucki W. J. et al., 2011a, ApJ, 728, 117

Borucki W. J. et al., 2011b, ApJ, 736, 19

Burke C. J., 2008, ApJ, 679, 1566

Butler R. P. et al., 2006, ApJ, 646, 505

Fischer D. A., Valenti J., 2005, ApJ, 622, 1102

Ford E. B., Rasio F. A., 2008, ApJ, 686, 621

Ford E. B., Quinn S. N., Veras D., 2008, ApJ, 678, 1407

Goldreich P., Soter S., 1966, Icarus, 5, 375

Howard A. W. et al., 2010, Sci, 330, 653

Johnson J. A., Aller K. M., Howard A. W., Crepp J. R., 2010, PASP, 122, 905

Jurić M., Tremaine S., 2008, ApJ, 686, 603

Kane S. R., von Braun K., 2008, ApJ, 689, 492

Kane S. R., von Braun K., 2009, PASP, 121, 1096

Kane S. R., Gelino D. M., 2012, PASP, 124, 323

Kipping D. M., 2008, MNRAS, 389, 1383

Lissauer J. J. et al., 2012, ApJ, 750, 112

Lissauer J. J. et al., 2011a, Nat, 470, 53

Lissauer J. J. et al., 2011b, ApJS, 197, 8

Lovis C. et al., 2011, A&A, 528, 112

Malmberg D., Davies M. B., 2009, MNRAS, 394, L26

Mandel K., Agol E., 2002, ApJ, 580, L171

Matsumura S., Takeda G., Rasio F. A., 2008, ApJ, 686, L29

Moorhead A. V. et al., 2011, ApJS, 197, 1

Plavchan P., Bilinski C., Currie T., 2012, ApJ, preprint (arXiv:1203.1887)

Pont F., Husnoo N., Mazeh T., Fabrycky D., 2011, MNRAS, 414, 1278

Seager S., Mallén-Ornelas G., 2003, ApJ, 585, 1038

Shen Y., Turner E. L., 2008, ApJ, 685, 553

Smalley B., 2005, Mem. Soc. Astron. Ital. Suppl., 8, 130

Terrien R. C., Mahadevan S., Bender C. F., Deshpande R., Ramsey L. W., Bochanski J. J., 2012, ApJ, 747, L38

von Braun K., Kane S. R., Ciardi D. R., 2009, ApJ, 702, 779

Wang J., Ford E. B., 2011, MNRAS, 418, 1822

Wright J. T. et al., 2011, PASP, 123, 412

Zakamska N. L., Pan M., Ford E. B., 2011, MNRAS, 410, 1895

This paper has been typeset from a $T_EX/I = T_EX$ file prepared by the author.